STEM CELLS TRANSLATIONAL MEDICINE®

TISSUE ENGINEERING AND REGENERATIVE MEDICINE

Multifaceted Therapeutic Benefits of Factors Derived From Dental Pulp Stem Cells for Mouse Liver Fibrosis

MARINA HIRATA,[a] MASATOSHI ISHIGAMI,[b] YOSHIHIRO MATSUSHITA,[a] TAKANORI ITO,[b] HISASHI HATTORI,[a] HIDEHARU HIBI,[a] HIDEMI GOTO,[b] MINORU UEDA,[a] AKIHITO YAMAMOTO[a]

Key Words. Liver fibrosis • Dental pulp stem cells • Conditioned media • Inflammation • Macrophages

[a]Department of Oral and Maxillofacial Surgery and [b]Department of Gastroenterology and Hepatology, Nagoya University Graduate School of Medicine, Nagoya, Japan

Correspondence: Akihito Yamamoto, D.D.Sc., Ph.D., 65 Tsurumai-cho, Showa-ku, Nagoya 466-8550, Japan. Telephone: 81-52-744-2348; E-Mail: akihito@med.nagoya-u.ac.jp

Received November 18, 2015; accepted for publication May 10, 2016; published Online First on June 8, 2016.

1066-5099/2016/$20.00/0

http://dx.doi.org/10.5966/sctm.2015-0353

ABSTRACT

Chronic liver injury from various causes often results in liver fibrosis (LF). Although the liver possesses endogenous tissue-repairing activities, these can be overcome by sustained inflammation and excessive fibrotic scar formation. Advanced LF leads to irreversible cirrhosis and subsequent liver failure and/or hepatic cancer. Here, using the mouse carbon tetrachloride (CCl_4)-induced LF model, we showed that a single intravenous administration of stem cells derived from human exfoliated deciduous teeth (SHEDs) or of SHED-derived serum-free conditioned medium (SHED-CM) resulted in fibrotic scar resolution. SHED-CM suppressed the gene expression of proinflammatory mediators, such as *TNF-α, IL-1β,* and *iNOS*, and eliminated activated hepatic stellate cells by inducing their apoptosis, but protected parenchymal hepatocytes from undergoing apoptosis. In addition, SHED-CM induced tissue-repairing macrophages that expressed high levels of the profibrinolytic factor, matrix metalloproteinase 13. Furthermore, SHED-CM suppressed the CCl_4-induced apoptosis of primary cultured hepatocytes. SHED-CM contained a high level of hepatocyte growth factor (HGF). Notably, HGF-depleted SHED-CM (dHGF-CM) did not suppress the proinflammatory response or resolve fibrotic scarring. Furthermore, SHED-CM, but not dHGF-CM, inhibited CCl_4-induced hepatocyte apoptosis. These results suggest that HGF plays a central role in the SHED-CM-mediated resolution of LF. Taken together, our findings suggest that SHED-CM provides multifaceted therapeutic benefits for the treatment of LF. STEM CELLS TRANSLATIONAL MEDICINE *2016;5:1416–1424*

SIGNIFICANCE

This study demonstrated that a single intravenous administration of stem cells from human exfoliated deciduous teeth (SHEDs) or of the serum-free conditioned medium (CM) derived from SHEDs markedly improved mouse liver fibrosis (LF). SHED-CM suppressed chronic inflammation, eliminated activated hepatic stellate cells by inducing their apoptosis, protected hepatocytes from undergoing apoptosis, and induced differentiation of tissue-repairing macrophages expressing high levels of the profibrinolytic factor matrix metalloproteinase 13. Furthermore, hepatocyte growth factor played a central role in the SHED-CM-mediated resolution of LF. This is the first report demonstrating the multifaceted therapeutic benefits of secreted factors derived from SHEDs for LF.

INTRODUCTION

Liver fibrosis (LF) is a consequence of many chronic liver diseases, such as viral infection and autoimmune hepatitis; alcohol abuse; and the use of certain drugs [1]. Chronic liver injury results in hepatocyte death by necrosis and apoptosis and in the subsequent activation of proinflammatory mediators, which promote the transdifferentiation of hepatic stellate cells (HSCs) into myofibroblasts. The activated HSCs or myofibroblasts synthesize extracellular matrix proteins that result in fibrotic scar formation. Severe liver fibrosis leads to the development of irreversible cirrhosis and subsequent liver failure [2]. Currently, the most effective cure for end-stage liver fibrosis is a liver transplant; however, because of the low supply of transplant donors, the development of a new cure is expected.

Recent studies have revealed that hepatic macrophages play central roles in both the progression and resolution of LF [3]. Diversity and plasticity are hallmarks of the monocyte/macrophage lineage. M1 and M2 macrophages are thought to represent the most polarized cells at either end of a continuum [4, 5]. M1 cells exhibit proinflammatory characteristics, whereas M2 cells counteract the proinflammatory M1-induced conditions and exhibit tissue-repairing activities [6]. During the injury phase of LF, M1 cells secrete high levels of inflammatory mediators, which induce the

profibrotic phenotype of HSCs. In contrast, restorative macrophages emerge during the resolution phase of LF and express high levels of matrix metalloproteinases (MMPs), whose activities degrade fibrotic scars and are required for the spontaneous recovery from carbon tetrachloride (CCl_4)-induced LF. These restorative macrophages exhibit unique properties, distinct from that of M2 cells [7, 8]. Proinflammatory monocytes recruited to the liver undergo a phenotypic switch, resulting in the differentiation into the restorative macrophages [9]. However, the mechanistic basis of this phenotypic switch is largely unknown.

Stem-cell therapy is a promising approach for the treatment of LF. Studies using the CCl_4-induced LF model in mice have shown that the transplantation or infusion of adult mesenchymal stem cells (MSCs) isolated from bone marrow (BMSCs) [10–13], umbilical cord [14, 15], adipose tissue (ADSCs) [16, 17], and amniotic mesenchymal tissues [18] reverses tissue destruction and fibrosis, primarily through paracrine mechanisms. However, some reports indicate that the infused MSCs can integrate into the injured liver and differentiate into myofibroblasts, thereby accelerating LF [19–21]. Thus, the careful examination must be required for the effects of MSC-transplantation therapy.

Stem cells secrete a broad range of trophic and immunomodulatory factors, which can be collected as serum-free conditioned medium (CM). Recent studies have shown that the factors derived from various types of stem cells have the potential for treating myriad intractable diseases [22]. In a study using the D-galactosamine-induced acute liver injury model in rats, the systemic administration of MSC-CM markedly improved the condition of the injured liver and the animals' survival rate [23–25]. However, the therapeutic effects of these stem cell-derived factors on LF are largely unknown.

Human adult dental pulp stem cells (DPSCs) and stem cells from human exfoliated deciduous teeth (SHEDs) are self-renewing MSCs residing within the perivascular niche of the dental pulp [26, 27]. These cells are thought to originate from the cranial neural crest, which expresses early markers for both MSCs and neuro-ectodermal stem cells [26–28]. Studies that evaluated engrafted SHEDs and DPSCs in various animal disease models indicate that these cells can promote significant recovery through paracrine mechanisms [29]. Intravenous administration of DPSCs has been shown to ameliorate CCl_4-induced LF [30]. Notably, we recently reported that SHED-CM treatments are therapeutically efficacious in various rodent disease models, such as ischemic brain injury [31, 32], Alzheimer's disease [33], spinal cord injury [34], fulminant liver failure [25], and bleomycin-induced fibrotic lung injury [35]. However, the therapeutic potential of SHED-CM for treating LF has not yet been examined.

Here we showed that CCl_4-induced LF mice treated with a single intravenous dose of SHED-CM exhibited remarkable recovery. Our data suggest that SHED-CM treatment would improve pathophysiology of LF by multifaceted therapeutic effects.

Materials and Methods

Isolation of SHEDs

SHEDs were isolated as previously described [28]. In brief, exfoliated deciduous teeth (from 6- to 12-year-old individuals), extracted for clinical purposes, were collected at Nagoya University School of Medicine using approved guidelines set by Nagoya University (H-73, 2003). Ethical approval was obtained from the ethics committee of Nagoya University (permission number 8-2). All participants provided written informed consent. After the crown and root were separated, the dental pulp was isolated and then digested in a solution containing 3 mg/ml collagenase type 1 and 4 mg/ml dispase for 1 hour at 37°C. Single-cell suspensions ($1–2 \times 10^4$ cells per milliliter) were plated on culture dishes in Dulbecco's modified Eagle's medium (DMEM) supplemented with 10% fetal calf serum, and then incubated at 37°C in 5% CO_2. Three human skin fibroblast lines (Fibros, derived from 36- to 40-year-old individuals) were obtained at passage 5 from the Health Science Research Resources Bank.

Preparation of CM

At passages 3–9, SHEDs or Fibro at 70%–80% confluence were washed with phosphate-buffered saline (PBS), and the culture medium was replaced with serum-free DMEM. After the cells were incubated for 48 hours, the medium was collected and centrifuged for 5 minutes at 1,500 rpm. The supernatant was then collected and centrifuged for 3 minutes at 3,000 rpm. The second supernatant was collected and used as the CM in subsequent experiments. To deplete the SHED-CM of hepatocyte growth factor (HGF) Protein-G Sepharose (GE Healthcare Life Sciences, Little Chalfont, United Kingdom, http://www.gelifesciences.com), prebound with an anti-HGF antibody (Ab), was added to the SHED-CM. The mixture was incubated for 1 hour at 4°C, and the Ab beads were then removed by centrifugation. The depletion procedure was repeated 3 more times. The absolute concentration of HGF in the CM was determined using an enzyme-linked immunosorbent assay kit (Quantikine ELISA Human HGF, R&D Systems, Minneapolis, MN, https://www.rndsystems.com/).

LF Induction in Mice and Treatment With SHEDs

Six-week-old female C57BL/6J mice from Japan SLC (Shizuoka, Japan, http://jslc.co.jp/english/index2.htm) were used for these experiments. LF was induced by biweekly intraperitoneal CCl_4 injections at 1.0 mg/kg during the course of 4 weeks. After 24 hours from the last CCl_4 injection, the following samples were injected into the jugular vein of the CCl_4-treated mice: (a) SHEDs (1.0×10^6), HGF (R&D Systems; 700 pg in 0.5 ml PBS) or the same volume of PBS, or (b) SHED-CM, Fibro-CM, or serum-free DMEM (0.5 ml). At 6, 12, or 24 hours after treatment, at least 5 animals per treatment group were sacrificed and the tissues were collected under deep anesthetized condition.

Real-Time Quantitative Polymerase Chain Reaction

Total RNA was quantified by a spectrophotometer, and RNA integrity was checked on 1% agarose gels. Reverse transcription reactions were carried out with Superscript III Reverse Transcriptase (Thermo Fisher Scientific Life Sciences, Waltham, MA, http://www.thermofisher.com) using 0.5 μg of total RNA in a 25-μl reaction volume. Real-time quantitative polymerase chain reaction (qPCR) was performed by using the THUNDERBIRD SYBR qPCR Mix (Toyobo, Osaka, Japan, http://www.toyobo-global.com) and the StepOnePlus Real-Time PCR System (Thermo Fisher Scientific Life Sciences). Mouse primers were designed using primer 3 (supplemental online Table 2).

Histological and Immunohistochemical Analysis

The animals were anesthetized and sacrificed 12 or 24 hours after SHED or SHED-CM infusion. Formalin-fixed, paraffin-embedded

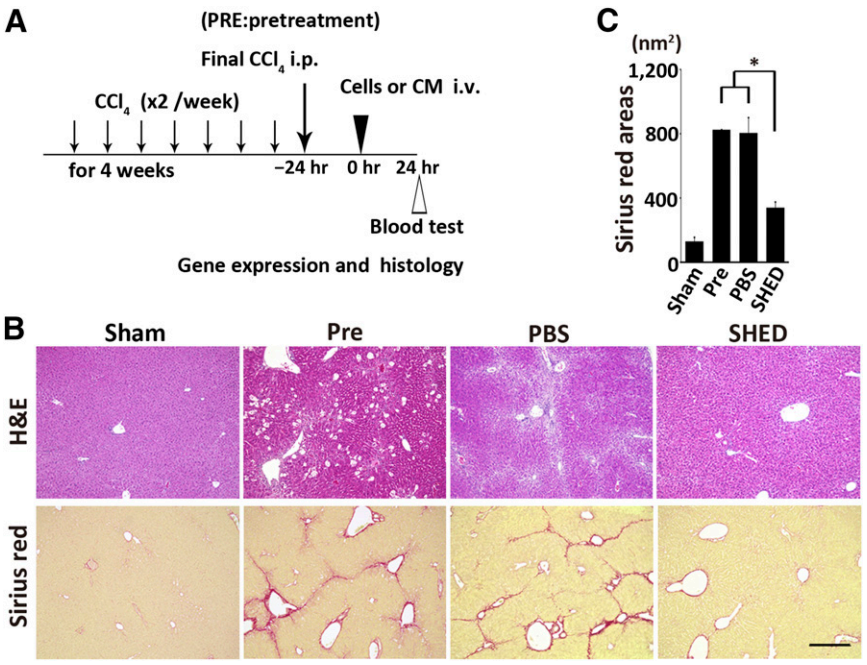

Figure 1. Therapeutic effects of SHEDs in mouse CCl_4-induced LF. **(A):** C57BL/6J mice were injected intraperitoneally with CCl_4 biweekly for 4 weeks. Twenty-four hours after the last injection, cells or CM were intravenously administered. Gene expression, histological, and blood analyses were carried out at the indicated time points. **(B):** Representative images of H&E and Sirius red-stained livers. Severe hepatocellular death with cytoplasmic vacuolization was observed throughout the Pre group. A single injection of SHEDs restored the normal liver structure. Scale bar = 300 μm. **(C):** Quantification of Sirius red-stained areas. $n = 4$ per group. Data represent mean ± SEM. *, $p < .05$. Abbreviations: CM, serum-free conditioned medium; H&E, hematoxylin and eosin; PBS, phosphate-buffered saline; Pre, pretreatment; SHED, stem cells derived from human exfoliated deciduous teeth.

liver samples were cut into 4-μm-thick sections and stained with hematoxylin-eosin (H&E) and Sirius red. For immunohistochemical analysis, the livers were embedded in optimal cutting temperature compound (Sakura Finetek, Torrance, CA, http://www.sakura-americas.com/) and cut into 4-μm-thick sections on a cryostat (Leica Biosystems, Wetzlar, Germany, http://www2.leicabiosystems.com). The sections were then permeabilized with 0.1% (vol/vol) Triton X-100 in PBS for 20 minutes, blocked with 5% (vol/vol) bovine serum albumin for 30 minutes, and incubated overnight with the following primary Abs: phycoerythrin-conjugated anti-CD11b (rat IgG, 1:500; eBioscience, San Diego, CA, http://www.ebioscience.com/), anti-MMP13 (rabbit IgG, 1:200; Abcam, Cambridge, United Kingdom, http://www.abcam.com/), or anti-collagen 1 (goat IgG, 1:200; Abcam). The following secondary Abs were used: anti-rabbit IgG-Alexa Fluor 647 and anti-goat IgG-Alexa Fluor 647. After counterstaining with 4′,6-diamidino-2-phenylindole (Sigma-Aldrich, St. Louis, MO, http://www.sigmaaldrich.com), the tissue images were captured with a universal fluorescence microscope (BZ9000, Keyence, Osaka, Japan, http://www.keyence.com). Apoptotic cell death was analyzed using the terminal deoxynucleotidyl transferase 2′-deoxyuridine 5′-triphosphate nick-end labeling (TUNEL) assay (In Situ Cell Death Detection Kit, Roche Life Science, Geneva, Switzerland, https://lifescience.roche.com). The collagen-stained areas with Sirius red or anti-collagen 1 Ab were quantified with ImageJ software (National Institutes of Health, Bethesda, MD, https://imagej.nih.gov/ij/). The average number of TUNEL/collagen 1-positive or MMP13/CD11b-positive cells per section was determined by counting 10 random fields in nonoverlapping sections at ×200 magnification. At least 3 animals per group were examined.

Bone Marrow Macrophage Assay

Bone marrow cells were isolated from 8-week-old female C57BL/6J mice. They were plated at 2×10^6 cells per 6-cm dish and differentiated into macrophages in DMEM supplemented with 20 ng/ml macrophage colony-stimulating factor (M-CSF) (Peprotech, Rocky Hill, NJ, https://www.peprotech.com), at 37°C in 5% CO_2 for 7 days. The macrophages were incubated with serum-free DMEM or SHED-CM for 24 hours, followed by mRNA analysis.

Hepatocyte Protection Assay

Hepatocytes were obtained as described previously [36]. In brief, the livers were perfused with liver perfusion medium (Thermo Fisher Scientific Life Sciences) at a flow rate of 3 ml/minute for 5 minutes. The livers were then perfused with basic perfusion solution (136 mM NaCl, 5.4 mM KCl, 5 mM $CaCl_2$, 0.5 mM NaH_2PO_3, 0.42 mM $Na_2HPO_3 \cdot 12H_2O$, 10 mM HEPES (pH 7.5), 5 mM glucose, and 4.2 mM $NaHCO_3$) containing 0.5 g/l collagenase type 4 (Yakult Pharmaceutical Industry Co., Ltd., Tokyo, Japan, http://www.yakult.co.jp/ypi/en/) at a flow rate of 3 ml/minute for 8 minutes. The digested livers were transferred to glass dishes containing Dulbecco's PBS and chopped into small pieces using a surgical knife. The extracted cells were dispersed by pipetting and were passed through a 70-μm cell strainer. After centrifugation at 500 rpm for 4 minutes, the cell pellet was suspended in an iso-osmotic Percoll solution and centrifuged at 600 rpm for 10 minutes. The pellet was then washed with DMEM, and single-cell suspensions ($1–2 \times 10^6$ cells per milliter) were plated on collagen 1-coated culture dishes. The isolated hepatocytes were stimulated with 86 μmol/l CCl_4 in SHED-CM or DMEM for 24 hours and then subjected to TUNEL analysis.

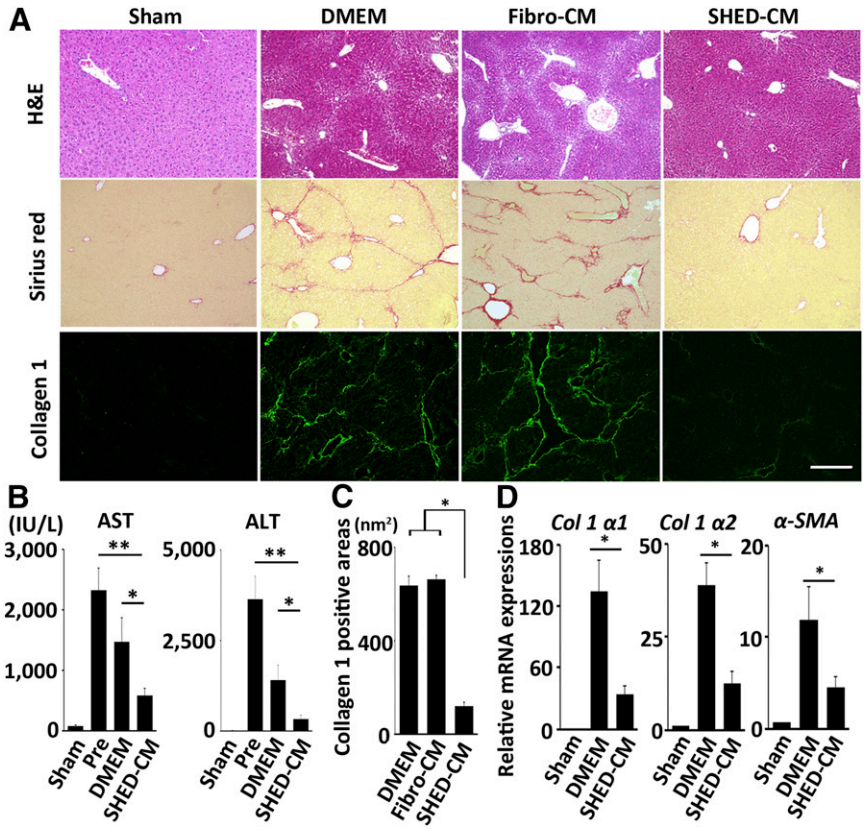

Figure 2. A single intravenous injection of SHED-CM ameliorates LF in mice. **(A):** Representative images of H&E, Sirius red, and collagen 1 immunofluorescence-stained livers. Scale bar = 300 μm. **(B and C):** Quantification of AST and ALT levels **(B)** and collagen 1-positive areas in the liver **(C)**. **(D)** Expression of *Col 1 α1* and *α2* and *α-SMA* mRNAs in the liver. Results are expressed relative to the level in the sham-operated (no CCl_4) mice. $n = 5$ per group. Data represent mean ± SEM. *, $p < .05$; **, $p < .01$. Abbreviations: ALT, alanine aminotransferase; AST, aspartate aminotransferase; CM, serum-free conditioned medium; DMEM, Dulbecco's modified Eagle's medium; Fibro, fibroblast line; H&E, hematoxylin and eosin; PBS, phosphate-buffered saline; Pre, pretreatment; SHED, stem cells derived from human exfoliated deciduous teeth; α-SMA, α-smooth muscle actin.

Statistical Analysis

All data are expressed as the mean ± SEM. Differences between groups were compared using repeated-measures analysis of variance with Tukey post hoc test (SPSS software, 19.0; IBM, Armonk, NY, http://www.ibm.com). A p value less than .05 was considered to indicate a statistically significant difference.

Results

Single Intravenous Injection of SHEDs Resolved CCl_4-Induced Liver Fibrosis

We evaluated the therapeutic benefits of SHEDs or SHED-CM for CCl_4-induced LF in mice (Fig. 1A). The SHEDs used in this study exhibited a fibroblastic morphology with a bipolar spindle shape; expressed MSC markers (CD90, CD73, and CD105) but not endothelial/hematopoietic markers (CD34, CD45, CD11b/c, or HLA-DR); and were capable of undergoing adipogenic, chondrogenic, and osteogenic differentiation [28]. There was no significant difference in the cellular survival of the SHEDs or fibroblasts after their incubation in serum-free versus serum-containing DMEM (data not shown).

Twenty-four hours after the eighth intraperitoneal administration of CCl_4 (subsequently referred to as pretreatment), prominent collagen accumulation and pseudolobule formation were evident (Fig. 1B). A single intravenous infusion of SHEDs resulted in LF resolution within 24 hours (Fig. 1B). Morphometric analysis using Sirius red staining revealed that the collagen 1-positive area of the livers in the SHED-treated group was about 40% of the area of the PBS or pretreatment groups (sham, 128.6 ± 22.1 nm^2; pretreatment, 821.7 ± 4.0 nm^2; PBS, 803.1 ± 95.4 nm^2; SHED, 339.3 ± 34.3 nm^2; $p < .05$ pretreatment vs. SHED, PBS vs. SHED) (Fig. 1B).

SHEDs Improved Liver Fibrosis by Paracrine Mechanisms

To analyze the paracrine activities of SHEDs, we harvested SHED-CM and examined its therapeutic effects on CCl_4-induced LF. Remarkably, a single intravenous injection of SHED-CM, but not of Fibro-CM or DMEM, resolved the LF and resulted in restoration of the normal liver structure (Fig. 2A). In the Fibro-CM-treated group, the degree of collagen accumulation and the expression of proinflammatory cytokines were equal to or greater than those of the DMEM-treated group (Fig. 2A; supplemental online Fig. 1). Thus, we used DMEM control thereafter. The alanine aminotransferase and aspartate aminotransferase levels in the peripheral blood were increased in the pretreatment group, whereas SHED-CM treatment significantly reduced those levels (Fig. 2B). Immunohistological analysis revealed that collagen 1-positive area in the liver of SHED-CM-treated mice was smaller than that of pretreatment, Fibro-CM-treated, or DMEM-treated mice (DMEM, 634.6 ± 40.9 nm^2; Fibro-CM, 662.8 ± 17.3 nm^2; SHED-CM, 120.2 ± 13.8 nm^2; $p <$ .01 DMEM vs. SHED-CM, Fibro-CM vs. SHED-CM) (Fig. 2C). In

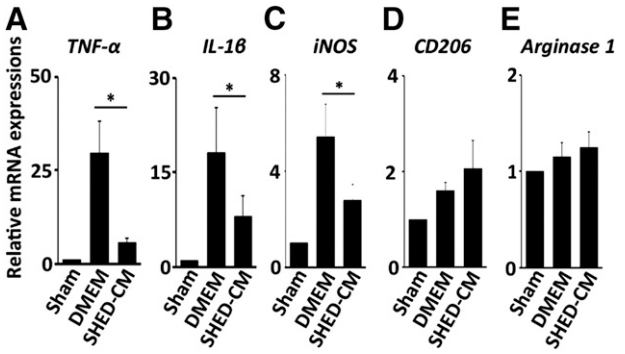

Figure 3. SHED-CM suppresses the proinflammatory M1 response. **(A–E):** Quantitative polymerase chain reaction analysis of the indicated mRNAs. Results are expressed relative to the level in the sham-operated mice. $n = 5$ per group. Data represent mean ± SEM. ∗, $p < .05$. Abbreviations: CM, serum-free conditioned medium; DMEM, Dulbecco's modified Eagle's medium; IL, interleukin; iNOS, inducible nitric oxide synthase; SHED, stem cells derived from human exfoliated deciduous teeth; TNF, tumor necrosis factor.

addition, qPCR analysis showed that SHED-CM treatment significantly suppressed the expression of the collagen type 1 (*Col 1 α1* and *α2*) and α-smooth muscle actin (*α-SMA*) mRNAs (Fig. 2D) ($p < .05$ for DMEM vs. SHED-CM for all mRNAs). Taken together, these results suggested that SHEDs improved the LF in mice, primarily through paracrine mechanisms.

SHED-CM Suppressed the Chronic Inflammatory Response in CCl_4-Treated Mice

Next, we examined the expression profile of mRNAs encoding pro- and anti-inflammatory cytokines and inducible nitric oxide synthase (*iNOS*) 24 hours after SHED-CM injection. *TNF-α*, *IL-1β*, and *iNOS* mRNAs were upregulated in the DMEM control group and were strongly suppressed by SHED-CM treatment (Fig. 3A–3C) ($p < .05$ for DMEM vs. SHED-CM for all genes). Although we previously reported that SHED-CM treatment induces the production of anti-inflammatory M2-like macrophages in D-galactosamine-induced acute liver failure in rats [25] and bleomycin-induced acute lung injury in mice [35], the elevation of the anti-inflammatory M2 type macrophage markers *CD206* and *Arginase 1* in SHED-CM-treated LF was marginal or not significant (Fig. 3D, 3E).

SHED-CM Induced Production of Restorative Hepatic Macrophages

Recent studies have highlighted an important role for restorative macrophages expressing MMP13 in the resolution of CCl_4-induced mouse LF [8]. Thus, we examined the temporal expression pattern of *MMP13* in the liver of CCl_4-treated mice after SHED-CM treatment. We found that the *MMP13* mRNA was markedly upregulated 6 hours after SHED-CM injection, exhibiting a 2.5-fold increase compared with the DMEM control (Fig. 4A) ($p < .05$ for DMEM vs. SHED-CM at all time points). Although the SHED-CM-induced *MMP13* level gradually decreased, it was still significantly higher than that in the DMEM control group 24 hours after treatment. Histological analysis of the liver 24 hours after SHED-CM or DMEM treatment showed that the number of $MMP13^+/CD11b^+$ cells in the SHED-CM-treated mice was 5 times that in the DMEM-treated mice (SHED-CM, 26.4% ± 1.1%; DMEM,

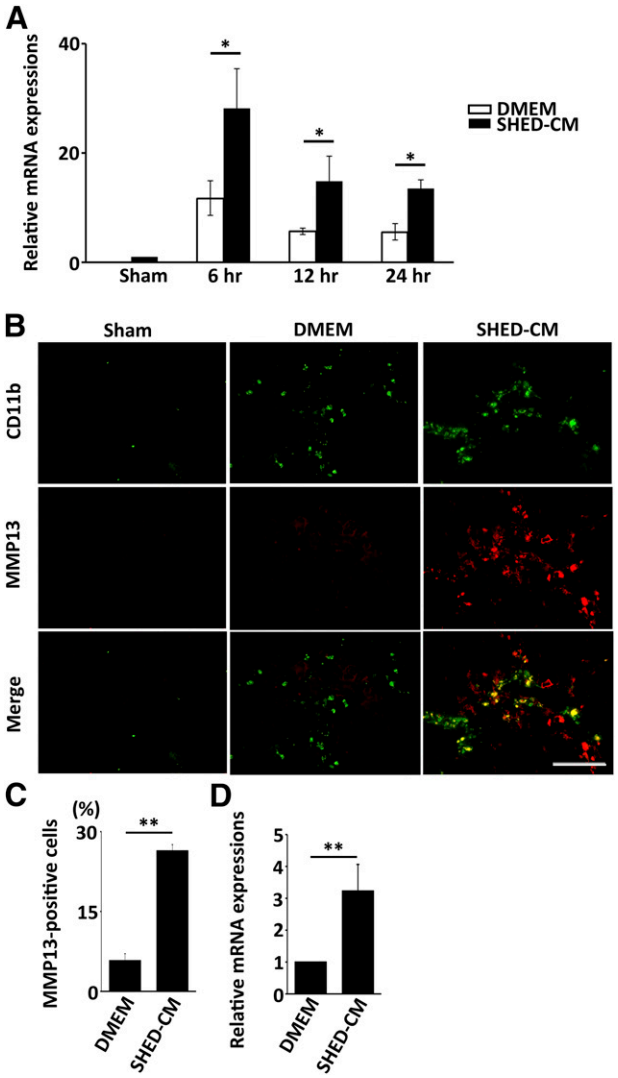

Figure 4. SHED-CM increases the polarization of macrophages expressing MMP13. **(A):** Changes in *MMP13* mRNA expression over time in the SHED-CM-treated and control mice. *MMP13* mRNA expression was strikingly upregulated 6 hours after SHED-CM injection. Results are expressed relative to the level in the sham-operated mice. $n = 5$ per group. Data represent mean ± SEM. ∗, $p < .05$. **(B):** Representative immunohistological staining images prepared 24 hours after SHED-CM injection. Scale bar = 100 μm. **(C):** Quantification of the $CD11b^+/MMP13^+$ hepatic macrophages. $n = 3$ per group. Data represent mean ± SEM. ∗, $p < .05$, ∗∗, $p < .01$, compared with the DMEM group. **(D):** The effect of SHED-CM on the *MMP13* expression in macrophages derived from bone marrow in vitro. Result is expressed relative to the level in DMEM group. $n = 6$ per group. Data represent the mean ± SEM. ∗∗, $p < .01$. Abbreviations: CM, serum-free conditioned medium; DMEM, Dulbecco's modified Eagle's medium; MMP, matrix metalloproteinase; SHED, stem cells derived from human exfoliated deciduous teeth.

5.7% ± 1.3%; $p < .01$) (Fig. 4B, 4C) and that these cells were associated with perilobular scar tissue.

Next, we examined whether SHED-CM could induce *MMP13* expression in macrophages derived from BM in vitro. Cells isolated from the BM were subjected to M-CSF treatment for 1 week to induce macrophages. The expression of *MMP13* in the SHED-CM-treated macrophages was 3.2 times that in the DMEM-treated macrophages (Fig. 4D) ($p < .05$ for DMEM vs. SHED-CM). These

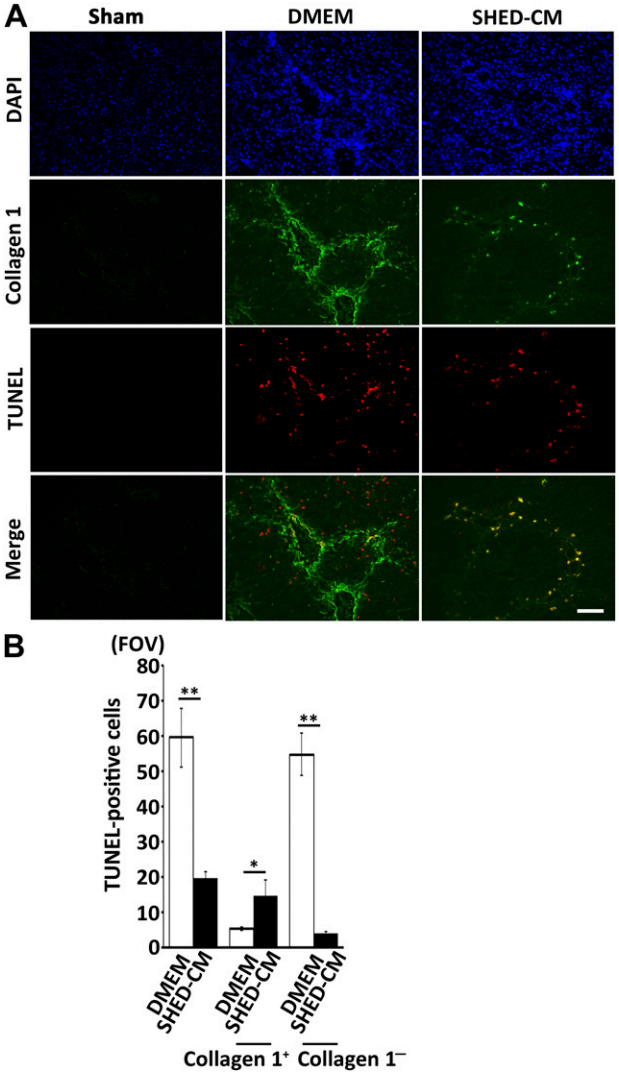

Figure 5. SHED-CM accelerates hepatic stellate cell apoptosis but protects hepatocytes. **(A):** Immunohistochemical staining and TUNEL analyses of liver sections prepared 12 hours after SHED-CM injection. Scale bar = 100 μm. **(B):** Quantification of the total number of TUNEL$^+$ cells, TUNEL$^+$/collagen 1$^+$ cells (apoptotic HSCs), and TUNEL$^+$/collagen 1$^-$ cells (apoptotic parenchymal hepatocytes). n = 4 per group. Data represent mean $\pm$ SEM. $*$, $p < .05$; $**$, $p < .01$ compared with the DMEM group. Abbreviations: CM, serum-free conditioned medium; DAPI, 4′,6-diamidino-2-phenylindole; DMEM, Dulbecco's modified Eagle's medium; FOV, field of view; SHED, stem cells derived from human exfoliated deciduous teeth; TUNEL, terminal deoxynucleotidyl transferase 2′-deoxyuridine 5′-triphosphate nick-end labeling.

results demonstrated that SHED-CM directly induced the polarization of restorative macrophages both in vivo and in vitro.

SHED-CM Accelerated HSC Apoptosis but Protected Hepatocytes

Immunofluorescent analysis revealed that the number of TUNEL$^+$ apoptotic cells in the DMEM group was about triple that of the SHED-CM group. Importantly, we found that the cell types of TUNEL$^+$ cells were different between these two groups. In the SHED-CM group, most TUNEL$^+$ cells were HSC-expressing collagen 1, whereas those in the DMEM group were hepatocytes located in the parenchymal hepatic lobule (supplemental online Fig. 2).

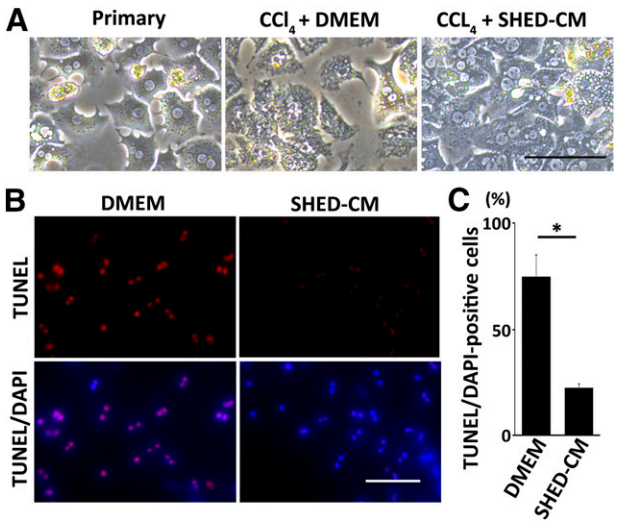

Figure 6. SHED-CM protects hepatocytes in vitro. **(A):** Phase contrast images of mouse hepatocytes stimulated with CCl_4 for 24 hours in the presence of DMEM or SHED-CM. Scale bar = 100 μm. **(B):** Representative images of hepatocyte TUNEL staining. Scale bar = 50 μm. **(C):** Quantification of the TUNEL$^+$/DAPI-stained hepatocytes. Data represent mean $\pm$ SEM. $*$, $p < .01$; $n = 3$ per group. Abbreviations: CM, serum-free conditioned medium; DAPI, 4′,6-diamidino-2-phenylindole; DMEM, Dulbecco's modified Eagle's medium; SHED, stem cells derived from human exfoliated deciduous teeth; TUNEL, terminal deoxynucleotidyl transferase 2′-deoxyuridine 5′-triphosphate nick-end labeling.

Statistical analysis showed that the number of TUNEL$^+$/collagen 1$^+$ cells (HSCs) in SHED-CM was 2.9 times higher than that of DMEM group (TUNEL$^+$/collagen 1$^+$ cells, 21.4 $\pm$ 3.9/field of view [FOV] in SHED-CM vs. 7.4 $\pm$ 1.6/FOV in DMEM control, $p < .05$) (Fig. 5B). In contrast, TUNEL$^+$/collagen 1$^-$ cells (hepatocytes) in SHED-CM group were 13.3 times lower than that of DMEM group (TUNEL$^+$/collagen 1$^-$ cells, 4.6 $\pm$ 0.3/FOV in SHED-CM vs. 59.9 $\pm$ 8.3/FOV in DMEM control; $p < .01$) (Fig. 5B). These results demonstrated that SHED-CM treatment induced HSC apoptosis but protected hepatocytes from undergoing apoptosis in CCl_4-induced LF.

Next, we examined the hepatocyte protection activity of SHED-CM in vitro. Hepatocytes were isolated from wild-type mouse liver and stimulated with CCl_4 in the presence of SHED-CM or DMEM. CCl_4 treatment induced hepatocyte apoptosis in DMEM, whereas apoptosis was significantly suppressed in SHED-CM (SHED-CM, 22.3% $\pm$ 1.9%; DMEM, 75.0% $\pm$ 10.2%, $p < .01$) (Fig. 6).

HGF Was Crucial for SHED-CM-Mediated Improvement of LF

Previous studies have revealed that HGF exerts multifaceted therapeutic effects in the treatment of both acute and chronic liver hepatitis [37–39]. To examine whether HGF is involved in the SHED-CM-mediated resolution of LF, we prepared HGF-depleted SHED-CM by treating the CM with Protein-G Sepharose prebound to an anti-HGF Ab, and designated as dHGF-CM (Fig. 7A). We also examined the therapeutic effect of HGF alone at the amount equal to SHED-CM. We found that both dHGF-CM and HGF alone (700 pg) failed to suppress the CCl_4-induced liver fibrosis, proinflammatory response, and α-*SMA* expression (Fig. 7B, 7C and supplemental online Fig. 3). dHGF-CM also failed to suppress the CCl_4-induced hepatocyte apoptosis in vitro (supplemental online Fig. 4). Although dHGF-CM was able to induce the MMP13$^+$ restorative macrophage as SHED-CM (supplemental online Fig. 5). Taken together, these results

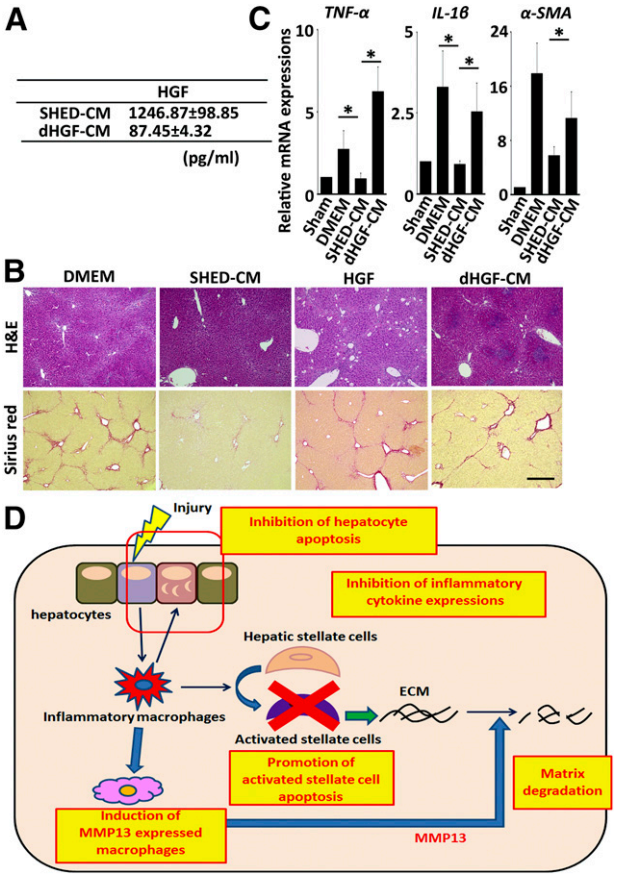

Figure 7. dHGF-CM fails to suppress the tissue destruction and chronic inflammation associated with liver fibrosis (LF). **(A):** Hepatocyte growth factor levels in SHED-CM and dHGF-CM were measured by enzyme-linked immunosorbent assay (n = 5 per group). Data represent the mean ± SEM. **(B):** Representative images of H&E- and Sirius red-stained liver sections. Scale bar = 300 μm. **(C):** Gene expression in the livers of DMEM-, dHGF-CM-, and SHED-CM-treated mice 24 hours after treatment. n = 5 per group. Results are expressed relative to the level in the sham-operated mice. Samples were isolated from 5 animals in each treatment group. Data represent the mean ± SEM. ∗, $p < .05$. **(D):** Postulated roles of SHED-CM in resolution of LF. Chronic liver injury results in hepatocyte death and subsequent activation of proinflammatory circumstances, which promote the transdifferentiation of hepatic stellate cells (HSCs) into myofibroblasts synthesizing ECM proteins. SHED-CM could restore LF through (a) inhibition of hepatocyte death, (b) suppression of proinflammatory response, (c) induction of the $MMP13^+$ restorative hepatic macrophages, and (d) elimination of the activated HSCs by inducing their apoptotic death. These multifaceted tissue-repairing activities would account for the resolution of LF. Abbreviations: CM, serum-free conditioned medium; dHGF, hepatocyte growth factor-depleted condition medium stem cells derived from human exfoliated deciduous teeth; DMEM, Dulbecco's modified Eagle's medium; ECM, extracellular matrix; H&E, hematoxylin and eosin; HGF, hepatocyte growth factor; IL, interleukin; MMP, matrix metalloproteinase; SHED, stem cells derived from human exfoliated deciduous teeth; α-SMA, α-smooth muscle actin; TNF, tumor necrosis factor.

demonstrated that HGF in SHED-CM was involved in the hepatocyte protection and played an essential role in the abrogation of LF.

Discussion

Numerous studies have reported that the intravenous administration of various types of stem cells improves LF by paracrine mechanisms [13, 14]. However, whether the application of stem cell-derived paracrine factors alone, without the cell graft, would promote significant recovery has been uncertain. Here, we report for the first time, to our knowledge, the therapeutic benefits of administering stem cell-derived CM for LF. Using the CCl_4-induced LF model in mice, we found that a single intravenous administration of SHED-CM was significantly more effective than Fibro-CM in improving the pathophysiology of LF. SHED-CM treatment suppressed the proinflammatory response of LF and induced the polarization of restorative hepatic macrophages, which expressed high levels of the profibrinolytic factor, MMP13. Furthermore, within 12 hours after administration, SHED-CM eliminated activated HSCs by inducing their apoptotic death but protected parenchymal hepatocytes from apoptosis (Fig. 7D). Thus, our data suggest that SHED-CM may provide significant therapeutic benefits for LF treatment.

We recently characterized the soluble factors in SHED-CM by cytokine Ab array analysis and found that it contained 79 of the array proteins at a level more than 1.5 times that in the control DMEM sample [34]. Here, we carried out a cluster analysis of these proteins and identified 11 that are known to exhibit functional properties that may be beneficial in treating LF (supplemental online Table 1). MMP10 is reported to have profibrinolytic effects in vivo due to its ability to enhance the fibrinolytic activity of tissue plasminogen activator. In acute and chronic liver injuries, mice lacking MMP10 exhibit severe liver fibrosis [40]. Vascular endothelial growth factor controls sinusoidal permeability, which facilitates the recruitment and infiltration of antifibrotic macrophages into scar tissue [41]. Studies using a rat cirrhosis model indicate that HGF administration induces the apoptosis of α-SMA-positive cells [39] while protecting parenchymal hepatocytes [37]. Stem cell factor inhibits the apoptosis and accelerates the proliferation of hepatocytes [42]. Interleukin-22, neuregulin 1, and insulin growth factor-binding protein-1 protect hepatocytes in various toxin-induced hepatic injury models [43–45]. Ferritin inhibits α-SMA expression [46]. Follistatin promotes liver regeneration after hepatectomy by facilitating DNA synthesis [47], and MCP-1 and ED-Siglec9 induce the polarization of anti-inflammatory/tissue-repairing macrophages [34]. The concentrations of these factors in SHED-CM may be low; however, we believe that the combinatorial effects of these factors in SHED-CM may provide therapeutic benefits for treating LF.

The clearance of HSCs by apoptosis is considered a potentially powerful therapeutic strategy for resolving fibrosis as well as cirrhosis [3, 48], and various pharmacological agents, such as gliotoxin, sulfasalazine, benzodiazepine ligands, curcumin, and tanshinone 1, have stimulated HSC apoptosis [49]. Although many of these agents have been tested in vitro, their therapeutic effects in LF remain largely unknown. Uniquely, gliotoxin, when administrated into the LF, stimulated HSC apoptosis and resolved fibrotic scar. However, gliotoxin also induced hepatocyte death at high concentrations, and no evidence demonstrates the restoration of liver function after gliotoxin treatment [50]. These data suggest that the clearance of HSC by apoptosis is not sufficient and other therapeutic effects would be required to restore liver function. Notably, our data showed that SHED-CM inhibited hepatocyte apoptosis both in vivo and in vitro, in addition to resolving fibrotic scarring by stimulating HSC apoptosis. Thus, SHED-CM is predicted to improve the liver function in LF through multifaceted effects.

Diversity and plasticity are hallmarks of the monocyte/macrophage lineage. M1 and M2 cells are thought to represent

the most polarized cells at either end of a continuum [4, 5]. Our previous studies demonstrated therapeutic effects of SHED-CM in D-galactosamine-induced acute liver failure models [25]. Notably, the therapeutic activities are associated with the SHED-CM-mediated conversion of proinflammatory M1-type disease microenvironments to anti-inflammatory M2 ones. In contrast, here we found that SHED-CM treatment induced the polarization of restorative macrophages that expressed high levels of MMP13 in CCl_4-induced LF. It has been reported that approximately half of restorative macrophages in LF are derived from a circulating pool of BM-derived monocytes [7]. Collectively, these findings suggest that SHED-CM has the potential to differentially affect macrophage polarization, depending on the underlying disease pathogenesis. In an acute model, D-galactosamine injection destroys liver, primarily through the recruitment and activation of the proinflammatory monocyte/macrophage lineages, whereas CCl_4 injection first induces the hepatocyte death and consequently activates inflammation. Thus, the severe inflammatory condition of acute liver failure may be required for SHED-CM-mediated M2 induction. It will be important to clarify the mechanistic basis of the SHED-CM-mediated macrophage regulation in each disease.

The therapeutic benefits and paracrine mechanisms associated with MSCs have drawn intense attention in the field of regenerative medicine. Nevertheless, their biological activities and the identities of the paracrine factors are largely unknown. HGF and adiponectin are considered promising therapeutic factors secreted from BMSCs and ADSCs or their derivatives [51, 52]. Previous studies showed that HGF and adiponectin induce similar tissue-repairing activities in various rodent disease models [53–58]. In LF, these factors inhibit the proinflammatory response, protect hepatocytes, and stimulate HSC apoptosis [37–39, 59, 60]. Our cytokine Ab array analysis revealed that SHED-CM contains high levels of HGF but little or no adiponectin. Therefore, we depleted the SHED-CM of HGF and examined the roles of HGF in the SHED-CM-mediated liver restoration. We found that dHGF-CM could no longer suppress the CCl_4-induced inflammatory response or induce fibrotic scar resolution. dHGF-CM failed to inhibit CCl_4-induced hepatocyte apoptosis. These results demonstrated that HGF in SHED-CM plays important roles in the SHED-CM-mediated functional recovery from LF. Notably, we recently reported that the HGF in SHED-CM inhibits myocardial apoptosis and reduces cardiac injury after ischemia-reperfusion in mice [61]. Thus, our studies demonstrate that HGF represents one of the central therapeutic factor in SHED-CM.

Conclusion

A single intravenous administration of SHED-CM improved the pathophysiology of CCl_4-induced LF. SHED-CM suppressed the chronic inflammatory response, eliminated activated HSCs by inducing their apoptotic death (but protected parenchymal hepatocytes), and promoted fibrinolysis by inducing the polarization of macrophages expressing MMP13. Our data suggest that SHED-CM may provide multifaceted therapeutic benefits for LF treatment.

Acknowledgments

We thank the Division of Experimental Animals and Medical Research Engineering, Nagoya University Graduate School of Medicine, for housing the animals and for microscope maintenance. This work was supported by Grants-in-Aid for Scientific Research on Priority Areas from the Ministry of Education, Culture, Sports, Science, and Technology of Japan.

Author Contributions

M.H.: conception and design, collection and/or assembly of data, data analysis and interpretation, manuscript writing; M.I., Y.M., and T.I.: collection and/or assembly of data, data analysis and interpretation; H. Hattori, H. Hibi, H.G., and M.U.: final approval of manuscript; A.Y.: conception and design, manuscript writing, final approval of manuscript.

Disclosure of Potential Conflicts of Interest

H.G. has compensated research funding from AbbVie GK; Fujifilm Holdings Corp.; Takara Bio Inc.; Bayer Yakuhin, Ltd., Taiho Pharmaceutical Co., Ltd.; Asahi Kasei Medical Co., Ltd.; Astellas Pharma Inc.; Kyowa Hakko Kirin Co., Ltd.; Takeda Pharmaceutical Company Ltd.; Otsuka Pharmaceutical Co., Ltd.; AstraZeneca K.K.; Mitsubishi Tanabe Pharma Corporation, Daiichi Sankyo Co., Ltd.; Eisai Co., Ltd.; Merck & Co., Inc.; Sumitomo Dainippon Pharma Co., Ltd.; and Bristol-Myers Squibb. The other authors indicated no potential conflicts of interest.

References

1 Friedman SL. Mechanisms of hepatic fibrogenesis. Gastroenterology 2008;134:1655–1669.
2 Bataller R, Brenner DA. Liver fibrosis. J Clin Invest 2005;115:209–218.
3 Pellicoro A, Ramachandran P, Iredale JP et al. Liver fibrosis and repair: Immune regulation of wound healing in a solid organ. Nat Rev Immunol 2014;14:181–194.
4 Mantovani A, Biswas SK, Galdiero MR et al. Macrophage plasticity and polarization in tissue repair and remodelling. J Pathol 2013;229:176–185.
5 Murray PJ, Allen JE, Biswas SK et al. Macrophage activation and polarization: Nomenclature and experimental guidelines. Immunity 2014;41:14–20.
6 Wynn TA, Ramalingam TR. Mechanisms of fibrosis: Therapeutic translation for fibrotic disease. Nat Med 2012;18:1028–1040.
7 Duffield JS, Forbes SJ, Constandinou CM et al. Selective depletion of macrophages reveals distinct, opposing roles during liver injury and repair. J Clin Invest 2005;115:56–65.
8 Fallowfield JA, Mizuno M, Kendall TJ et al. Scar-associated macrophages are a major source of hepatic matrix metalloproteinase-13 and facilitate the resolution of murine hepatic fibrosis. J Immunol 2007;178:5288–5295.
9 Ramachandran P, Pellicoro A, Vernon MA et al. Differential Ly-6C expression identifies the recruited macrophage phenotype, which orchestrates the regression of murine liver fibrosis. Proc Natl Acad Sci USA 2012;109:E3186–E3195.
10 Zhao DC, Lei JX, Chen R et al. Bone marrow-derived mesenchymal stem cells protect against experimental liver fibrosis in rats. World J Gastroenterol 2005;11:3431–3440.
11 Abdel Aziz MT, Atta HM, Mahfouz S et al. Therapeutic potential of bone marrow-derived mesenchymal stem cells on experimental liver fibrosis. Clin Biochem 2007;40:893–899.
12 Chang YJ, Liu JW, Lin PC et al. Mesenchymal stem cells facilitate recovery from chemically induced liver damage and decrease liver fibrosis. Life Sci 2009;85:517–525.
13 Miryounesi M, Piryaei A, Pournasr B et al. Repeated versus single transplantation of mesenchymal stem cells in carbon tetrachloride-induced liver injury in mice. Cell Biol Int 2013;37:340–347.
14 Tsai PC, Fu TW, Chen YMA et al. The therapeutic potential of human umbilical mesenchymal stem cells from Wharton's jelly in the treatment of rat liver fibrosis. Liver Transpl 2009;15:484–495.
15 Jung KH, Shin HP, Lee S et al. Effect of human umbilical cord blood-derived mesenchymal stem cells in a cirrhotic rat model. Liver Int 2009;29:898–909.
16 Yu F, Ji S, Su L et al. Adipose-derived mesenchymal stem cells inhibit activation of hepatic stellate cells in vitro and ameliorate rat liver fibrosis in vivo. J Formos Med Assoc 2015;114:130–138.
17 Wang Y, Lian F, Li J et al. Adipose derived mesenchymal stem cells transplantation via

portal vein improves microcirculation and ameliorates liver fibrosis induced by CCl4 in rats. J Transl Med 2012;10:133.

18 Zhang D, Jiang M, Miao D. Transplanted human amniotic membrane-derived mesenchymal stem cells ameliorate carbon tetrachloride-induced liver cirrhosis in mouse. PLoS One 2011;6:e16789.

19 Kisseleva T, Brenner DA. The phenotypic fate and functional role for bone marrow-derived stem cells in liver fibrosis. J Hepatol 2012;56:965–972.

20 Baertschiger RM, Serre-Beinier V, Morel P et al. Fibrogenic potential of human multipotent mesenchymal stromal cells in injured liver. PLoS One 2009;4:e6657.

21 di Bonzo LV, Ferrero I, Cravanzola C et al. Human mesenchymal stem cells as a two-edged sword in hepatic regenerative medicine: Engraftment and hepatocyte differentiation versus profibrogenic potential. Gut 2008;57:223–231.

22 Ranganath SH, Levy O, Inamdar MS et al. Harnessing the mesenchymal stem cell secretome for the treatment of cardiovascular disease. Cell Stem Cell 2012;10:244–258.

23 Parekkadan B, van Poll D, Suganuma K et al. Mesenchymal stem cell-derived molecules reverse fulminant hepatic failure. PLoS One 2007;2:e941.

24 van Poll D, Parekkadan B, Cho CH et al. Mesenchymal stem cell-derived molecules directly modulate hepatocellular death and regeneration in vitro and in vivo. Hepatology 2008;47:1634–1643.

25 Matsushita Y, Ishigami M, Matsubara K et al. Multifaceted therapeutic benefits of factors derived from stem cells from human exfoliated deciduous teeth for acute liver failure in rats. J Tissue Eng Regen Med 2015 [Epub ahead of print].

26 Gronthos S, Mankani M, Brahim J et al. Postnatal human dental pulp stem cells (DPSCs) in vitro and in vivo. Proc Natl Acad Sci USA 2000; 97:13625–13630.

27 Miura M, Gronthos S, Zhao M et al. SHED: Stem cells from human exfoliated deciduous teeth. Proc Natl Acad Sci USA 2003;100:5807–5812.

28 Sakai K, Yamamoto A, Matsubara K et al. Human dental pulp-derived stem cells promote locomotor recovery after complete transection of the rat spinal cord by multiple neuro-regenerative mechanisms. J Clin Invest 2012;122:80–90.

29 Yamamoto A, Sakai K, Matsubara K et al. Multifaceted neuro-regenerative activities of human dental pulp stem cells for functional recovery after spinal cord injury. Neurosci Res 2014;78:16–20.

30 Ikeda E, Yagi K, Kojima M et al. Multipotent cells from the human third molar: Feasibility of cell-based therapy for liver disease. Differentiation 2008;76:495–505.

31 Yamagata M, Yamamoto A, Kako E et al. Human dental pulp-derived stem cells protect against hypoxic-ischemic brain injury in neonatal mice. Stroke 2013;44:551–554.

32 Inoue T, Sugiyama M, Hattori H et al. Stem cells from human exfoliated deciduous tooth-derived conditioned medium enhance recovery of focal cerebral ischemia in rats. Tissue Eng Part A 2013;19:24–29.

33 Mita T, Furukawa-Hibi Y, Takeuchi H et al. Conditioned medium from the stem cells of human dental pulp improves cognitive function in a mouse model of Alzheimer's disease. Behav Brain Res 2015;293:189–197.

34 Matsubara K, Matsushita Y, Sakai K et al. Secreted ectodomain of sialic acid-binding Ig-like lectin-9 and monocyte chemoattractant protein-1 promote recovery after rat spinal cord injury by altering macrophage polarity. J Neurosci 2015;35:2452–2464.

35 Wakayama H, Hashimoto N, Matsushita Y et al. Factors secreted from dental pulp stem cells show multifaceted benefits for treating acute lung injury in mice. Cytotherapy 2015; 17:1119–1129.

36 Okabe M, Tsukahara Y, Tanaka M et al. Potential hepatic stem cells reside in EpCAM+ cells of normal and injured mouse liver. Development 2009;136:1951–1960.

37 Valdés-Arzate A, Luna A, Bucio L et al. Hepatocyte growth factor protects hepatocytes against oxidative injury induced by ethanol metabolism. Free Radic Biol Med 2009;47: 424–430.

38 Mizuno S, Nakamura T. Hepatocyte growth factor: A regenerative drug for acute hepatitis and liver cirrhosis. Regen Med 2007;2:161–170.

39 Kim WH, Matsumoto K, Bessho K et al. Growth inhibition and apoptosis in liver myofibroblasts promoted by hepatocyte growth factor leads to resolution from liver cirrhosis. Am J Pathol 2005;166:1017–1028.

40 Garcia-Irigoyen O, Carotti S, Latasa MU et al. Matrix metalloproteinase-10 expression is induced during hepatic injury and plays a fundamental role in liver tissue repair. Liver Int 2014;34:e257–e270.

41 Shimizu H, Miyazaki M, Wakabayashi Y et al. Vascular endothelial growth factor secreted by replicating hepatocytes induces sinusoidal endothelial cell proliferation during regeneration after partial hepatectomy in rats. J Hepatol 2001;34:683–689.

42 Hu B, Colletti LM. Stem cell factor and c-kit are involved in hepatic recovery after acetaminophen-induced liver injury in mice. Am J Physiol Gastrointest Liver Physiol 2008; 295:G45–G53.

43 Zenewicz LA, Yancopoulos GD, Valenzuela DM et al. Interleukin-22 but not interleukin-17 provides protection to hepatocytes during acute liver inflammation. Immunity 2007;27:647–659.

44 Dorsey WC, Tchounwou PB, Ford BD. Neuregulin 1-Beta cytoprotective role in AML 12 mouse hepatocytes exposed to pentachlorophenol. Int J Environ Res Public Health 2006;3:11–22.

45 Leu JI, Crissey MA, Taub R. Massive hepatic apoptosis associated with TGF-beta1 activation after Fas ligand treatment of IGF binding protein-1-deficient mice. J Clin Invest 2003;111: 129–139.

46 Ramm GA, Britton RS, O'Neill R et al. Rat liver ferritin selectively inhibits expression of alpha-smooth muscle actin in cultured rat lipocytes. Am J Physiol 1996;270:G370–G375.

47 Kogure K, Zhang YQ, Kanzaki M et al. Intravenous administration of follistatin: delivery to the liver and effect on liver regeneration after partial hepatectomy. Hepatology 1996; 24:361–366.

48 Trautwein C, Friedman SL, Schuppan D et al. Hepatic fibrosis: Concept to treatment. J Hepatol 2015;62(Suppl):S15–S24.

49 Elsharkawy AM, Oakley F, Mann DA. The role and regulation of hepatic stellate cell apoptosis in reversal of liver fibrosis. Apoptosis 2005;10:927–939.

50 Orr JG, Leel V, Cameron GA et al. Mechanism of action of the antifibrogenic compound gliotoxin in rat liver cells. Hepatology 2004;40: 232–242.

51 Nagaya N, Kangawa K, Itoh T et al. Transplantation of mesenchymal stem cells improves cardiac function in a rat model of dilated cardiomyopathy. Circulation 2005; 112:1128–1135.

52 Kilroy GE, Foster SJ, Wu X et al. Cytokine profile of human adipose-derived stem cells: Expression of angiogenic, hematopoietic, and pro-inflammatory factors. J Cell Physiol 2007;212:702–709.

53 Ohashi K, Kihara S, Ouchi N et al. Adiponectin replenishment ameliorates obesity-related hypertension. Hypertension 2006; 47:1108–1116.

54 Miyagawa S, Sawa Y, Taketani S et al. Myocardial regeneration therapy for heart failure: Hepatocyte growth factor enhances the effect of cellular cardiomyoplasty. Circulation 2002;105:2556–2561.

55 Gong R, Rifai A, Tolbert EM et al. Hepatocyte growth factor ameliorates renal interstitial inflammation in rat remnant kidney by modulating tubular expression of macrophage chemoattractant protein-1 and RANTES. J Am Soc Nephrol 2004;15:2868–2881.

56 Koike H, Morishita R, Iguchi S et al. Enhanced angiogenesis and improvement of neuropathy by cotransfection of human hepatocyte growth factor and prostacyclin synthase gene. FASEB J 2003;17:779–781.

57 Maruyama S, Shibata R, Ohashi K et al. Adiponectin ameliorates doxorubicin-induced cardiotoxicity through Akt protein-dependent mechanism. J Biol Chem 2011;286:32790–32800.

58 Xu A, Wang Y, Keshaw H et al. The fat-derived hormone adiponectin alleviates alcoholic and nonalcoholic fatty liver diseases in mice. J Clin Invest 2003;112:91–100.

59 Sennello JA, Fayad R, Morris AM et al. Regulation of T cell-mediated hepatic inflammation by adiponectin and leptin. Endocrinology 2005;146:2157–2164.

60 Moschen AR, Wieser V, Tilg H. Adiponectin: Key player in the adipose tissue-liver crosstalk. Curr Med Chem 2012;19:5467–5473.

61 Yamaguchi S, Shibata R, Yamamoto N et al. Dental pulp-derived stem cell conditioned medium reduces cardiac injury following ischemia-reperfusion. Sci Rep 2015;5:16295.

See www.StemCellsTM.com for supporting information available online.